Bioelectrochemistry 146 (2022) 108164

Contents lists available at ScienceDirect

Bioelectrochemistry

journal homepage: www.journals.elsevier.com/bioelectrochemistry

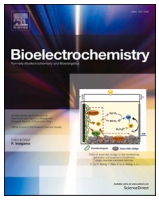

Electrocatalytic enhancement of $[Ru(bpy)_3]^{2+}$ electrochemiluminescence for gemcitabine detection toward precision measurement via gold nanoparticle addition

Kelly Brown, Adeolu Oluwasanmi, Clare Hoskins, Lynn Dennany

WestCHEM, Department of Pure and Applied Chemistry, University of Strathclyde, Technology & Innovation Centre, 99 George Street, Glasgow G1 1RD, UK

ARTICLE INFO

Keywords:
Electrochemiluminescence
Precision medicine
Electrocatalytic enhancement
Gold nanoparticles

ABSTRACT

With a rise in the development and subsequent employment of precision medicine, their lies an immediate necessity for the development of technology to enable the implementation of such treatment plans into the healthcare environment. Electrochemistry stands to offer one of the most viable techniques for such technologies given its success within current medical devices. One electrochemical technique, electrochemiluminescence (ECL), warrants investigation. Previously we have determined the inability to reliably detect cancer therapy gemcitabine via traditional ruthenium based ECL. Here we demonstrate how the addition of gold nanoparticles into the ECL film can promote GMB detection via enhanced electrocatalytic oxidation, generating the required ECL radicals. Via this approach we have been able to improve the ECL signal intensity 60-fold and achieve detection down to 6.25 μM across a linear range of 6.25–50 μM. Which lies within the therapeutically relevant range. This approach has successfully addressed the prior limitations encountered for the employment of traditional ruthenium based ECL for substance identification, where species exhibit limited electro-activity and suffer from electrochemically induced side reactions.

1. Introduction

Precision medicine has been identified as the next major development in regard to world healthcare approaches and will seek to introduce a tailored approach toward patient care and offer a replacement of the current "one size fits all" treatment strategy [1–4]. Tailored treatment approaches will see treatment plans developed based upon a patients disease specific characteristics with the ultimate goal to minimise side effects and increase treatment efficacy. In order to implement such ambitious treatment plans, it will become key to ensure real-time monitoring of a patient's response is possible. To achieve this, recording disease specific biomarkers and blood circulating concentrations of treatment therapies in the first instance will be required [1–4]. Examining these characteristics will aid clinicians to adjust the effective dosage in real time, minimising any adverse side effects toward healthy tissues and cells by adjustment with regard to biomarker fluctuations. While the fundamental groundwork toward personalised medicine is available, the current healthcare systems lack the required resources and necessary technology to implement the ambitious plans across a wide range of disease types. The development of continuous monitoring sensors for this avail is not unattainable, in fact the foundations are already present through the commercially available continuous blood glucose monitors for diabetic patients, which provides them with real-time readings altering them when to administer insulin etc. [5,6].

Expanding upon the success of electrochemical sensors within medical devices, sensors employing alternative electrochemical techniques such as electrochemiluminescence (ECL) offer new possibilities. ECL employment has received increasing interest within the bio-analytical and bio-medical fields within recent years, likely attribute to the undeniable benefits it offers, including portability and high sensitivity couple with operational simplicity [7–16]. Despite this the employment of ECL within the clinical arena is largely negligible, likely related to a limited knowledge outwith the electro-analytical chemistry field of the technique and the advantages it offers. The lack of wider knowledge of ECL, even within the electrochemical field, does see its use associated with a single luminophore and a lack of specificity. Previously we have shown an initial concept proof for the detection of a cancer therapeutic agent via ECL [17]. Gemcitabine (GMB), is a widely employed nucleoside analogue used in the treatment of various carcinomas including non-small cell lung, pancreatic, metastatic breast and recurrent ovarian cancer [18–21]. With oncology one of the major areas which would benefit from personalised medicine, it seems pertinent to

E-mail address: lynn.dennany@strath.ac.uk (L. Dennany).

https://doi.org/10.1016/j.bioelechem.2022.108164
Received 25 February 2022; Received in revised form 12 May 2022; Accepted 15 May 2022
Available online 20 May 2022

begin development toward a monitoring device relevant to this area. GMB has demonstrated satisfactory electro-activity, making it ideal as a model compound for development [22–24].

Previously, we have reported on the inability to effectively detect GMB at clinically relevant concentrations with the typical ruthenium luminophore $[Ru(bpy)_3]^{2+}$; due to its limited electro-activity and competing dimerisation reactions reducing the number of available radicals to proceed down the ECL pathway [17]. Within this contribution we offer an alternative strategy to overcome this prior limitation through the employment of gold nanoparticles offering an electrode surface capable of catalytically oxidising a higher portion of the GMB species present, with the aim to facilitate GMB detection via ECL. This will improve the outlook of ECL for employment within personalised oncology and offering a simpler ECL strategy than previously proposed.

2. Reagents & Apparatus

2.1. Materials & chemicals

Gemcitabine hydrochloride (GMB), leucovorin calcium (LV), tris (2,2′-bipyridyl) - (dichlororuthenium (II) hexahydrate ($[Ru(bpy)_3]^{2+}$), sodium chloride (NaCl), 20 nM gold nanoparticles (AuNP) stabilised in citrate buffer and 117 Nafion (~5% mixture of lower aliphatic alcohols) were purchased from Sigma Aldrich. All chemicals were used as received and all solutions prepared in Milli-Q (18 MΩ cm^{-1}).

2.2. Inductively coupled plasma – optical emission spcectrscopy (ICP-OES)

AuNP samples for ICP-OES were acid digested in 1:1 v/v hydrochloric: nitric acid solution. Once fully digested samples were diluted with Milli-Q and analysed for Au (242.794) content using a Agilent Technologies 700 series system.

2.3. Transmission electron microscopy (TEM)

TEM was performed upon 20 μL of the AuNP dispersion. For analysis samples were pipetted onto formvar copper grids and left to air dry. TEM's were performed using a JEOL JEM-1230, where scans were performed over a large area and a representative image was obtained.

2.4. Electrochemical analysis

All electrochemical and corresponding photoluminescence measurements were performed through the coupling of a PalmSens 4 potentiostat to a Hamamatsu H10723-20 photomultiplier tube (PMT). All of which was housed within a light tight Faraday cage. Photoluminescence measurements were performed via a specially designed sensor holder which positions the PMT window directly above the working electrode surface. All measurements were performed upon custom screen-printed electrodes (SPE) from Flexmedical Solutions, incorporating a 5 mm carbon working electrode, carbon counter and a quasi-silver paste reference.

2.5. ECL sensor fabrication

The ECL sensor was fabricated via modification to our previously published procedure [17,25,26]. In brief, this encompassed the drop casting of a mixture containing a predetermined ratio of AuNP (either 1:1 v/v or 2:1 v/v) to 0.5 mM of the $[Ru(bpy)_3]^{2+}$ complex encapsulated within a 0.2% Nafion conductive film. Once cast to avoid any degradation to the carbon working surface, heat was gently applied to ensure swift evaporation off any residual solvent and secure the complex to the electrode surface.

3. Results

3.1. Electrochemical behaviour of GMB

We have previously investigated the electrochemical behaviour of GMB upon these screen printed carbon paste working electrodes, which revealed GMB possessed relatively poor electrochemical behaviour upon this material with the expected oxidation peak only observed at significantly high concentrations of 0.5 mM and above [17]. As demonstrated within Fig. 1 (a), this remains true with the single expected oxidation peak, attributed to oxidation of the amine moiety within GMB, not observed at lower concentrations with a indistinguishable peak form the background charging current observed. Yet GMB has previously shown significant electro-activity upon gold working electrodes with detection limits down to as low as 0.06 μM [23,24]. Analysis of GMB upon gold SPE revealed an irreversible oxidation peak at ~ 0.94 V (vs Ag) (Fig. 1 (b)) indicating GMB displays an enhanced electro-activity at a gold electrode surface. The appearance of this irreversible oxidation peak upon the gold electrode is in line with those previously reported [23,24] and relates to oxidation of the secondary amine moiety. As with other prior studies it remains necessary for samples to be pH adjusted to alkaline values to maximise the number of de-protonated GMB molecules, which are converted to this electroactive form for detection. The appearance of the oxidation peak upon the gold working electrode surface likely relates to the far greater electron-transfer rate upon this material promoting the direct oxidation of GMB, in a similar manner to that reported for other electroactive compounds of interest [27]. However, the utilisation of bulk gold electrodes toward ECL prognostic point-of-care devices is intrinsically unsuited. Not only are gold electrodes significantly higher cost than their carbon counter parts (an aspect which keeping to a minimum would be beneficial within the medical arena), it is also well accepted that ECL upon bulk gold working electrodes is highly limited as a consequence of the quenching effects seen from the inhibition of amine oxidation due to the gold surface oxides produced during the potential sweep [28,29]. This can be confirmed through interrogation of the ECL signal observed upon the bulk gold electrodes (Fig. 1 (c)), which despite the CV demonstrating the effective oxidation of GMB, producing the required radical for the ECL pathway to proceed, no emission was observed. This contrasts with the notable signal produced at the same concentration upon the bare carbon working electrode, indicating we are indeed observing a quenching effect upon the ECL emission at the gold working electrode surface.

3.2. Impact of the addition of AuNP to the electrochemical behaviour of GMB

A comprise between the aforementioned competing effects however can be reached through the utilisation of gold nanoparticles (AuNP). The employment of AuNP upon the electrode surface would provide a significant increase in the available electroactive area, hence promoting the electrocatalytic oxidation of GMB. However, AuNP do not produce the same ECL quenching effects as observed upon bulk gold electrodes. ECL enhancement via the addition of AuNP to a bare electrode surface has been previously demonstrated to great effect by the groups of Chen et al. [30], Dong et al. [31] and Xu et al. [32] all whom reported a significant increase in ECL signal intensity upon inclusion of AuNP to their electrode surfaces (a trend replicated here see Fig. 3 (b)) [30–32]. The AuNP were characterised prior to inclusion upon the electrode surface via TEM and ICP-OES. These revealed the spherical AuNP possessed a similar size to 20 nm (refer to Figure S1) with a Au metal content of 0.103 mg mL^{-1} (102 ppm). The intrinsic electrochemical behaviour of the AuNP was initially investigated prior to subsequent immobilisation upon the carbon working electrode. This revealed a number of anodic peaks in line with those previously reported to relate to the oxidation of AuNP with two unresolved anodic peaks at ~ 0.1 V and ~ 0.3 V vs Ag respectively and a larger anodic peak observed at ~

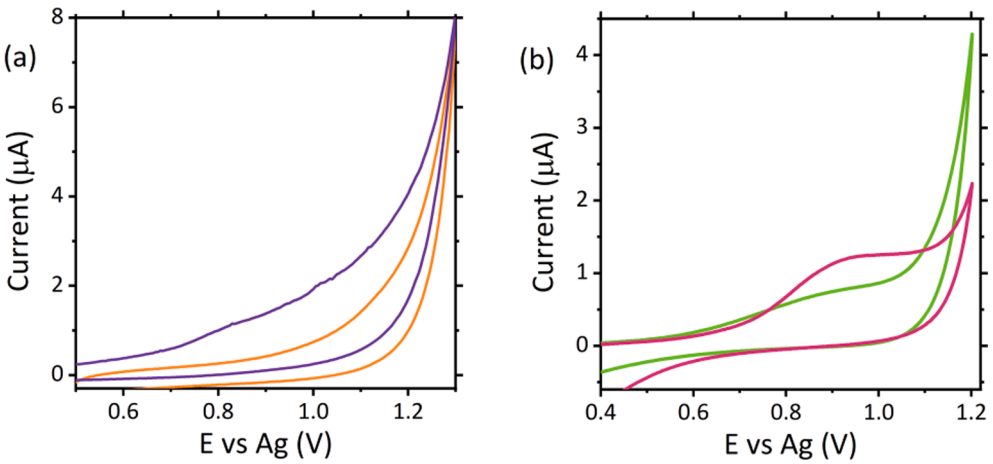

Fig. 1. (a) CV of 0.1 mM GMB (purple), and 0.1 M NaCl only (orange) obtained from a carbon paste SPE (working electrode) with a supporting electrolyte of 0.1 M NaCl (b) CV of 0.1 mM GMB (pink) obtained from a gold SPE (working electrode) with a supporting electrolyte of 0.1 M NaCl, control NaCl is shown by the green trace and (c) ECL signals of 0.5 mM GMB obtained from carbon (blue) and gold (pink) SPE (working electrode) with 0.1 M NaCl (green) as the supporting electrolyte. All measurements were collected at a scan rate of 100 mV s^{-1} across a potential range of $0.2 \leq E \geq 1.25$ V vs. Ag with a PMT bias of 0.6 V for (c).

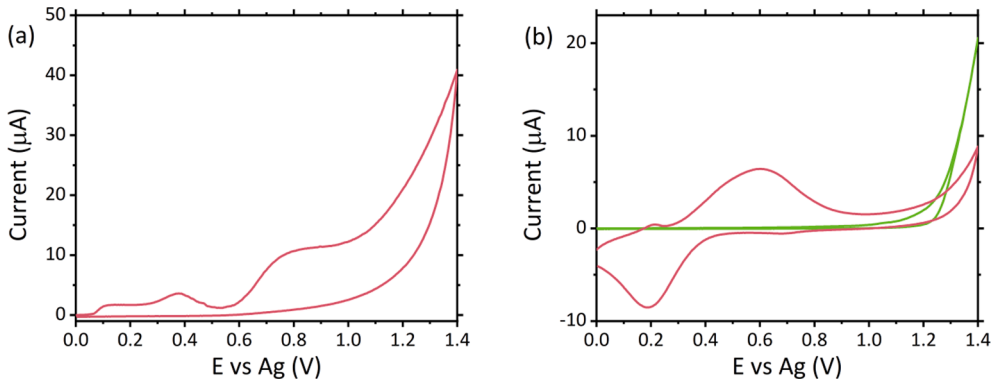

Fig. 2. Typical CV response of (a) the AuNP stock solution and (b) AuNP when immobilised upon the carbon working electrode (pink) compared with a bare electrode (green), where a supporting electrolyte of 0.1 M NaCl was used, measurements were collected at a scan rate of 100 mV s-1 across a potential range of $0 \leq E \geq 1.4$ V vs. Ag.

0.8 V, see Fig. 2 (a) [31,33]. Here immobilisation of the AuNP to the carbon surface was performed via a simple drop-casting method using the conductive polymer Nafion, avoiding the need for any self-assembly or deposition mechanisms was performed. Reproducibility of the surface modification procedure was determined as sufficient with an %RSD of 3.4, 4 and 5.4 % across i_{Pa}, i_{Pc} and maximum ECL intensity, at n = 3, refer to Figure S2. The presence of the AuNP upon the electrode surface was confirmed via interrogation of the CV shown within Fig. 2 (b), where the large oxidation peak is observed at ~ 0.6 V vs Ag, and a reduction peak is seen at ~ 0.2 V vs Ag, neither of which are seen upon bare carbon electrodes. The appearance of the reduction peak following surface immobilisation, likely arises due to the close proximity of the AuNP to the electrode surface. This reduction peak is typical of AuNP fixed upon an electrode surface and thus is intrinsic to the system, and can be used to confirm successful fixation of the AuNP to the working electrode surface [27,29–31,33]. Immobilisation of the AuNP to the electrode surface resulted in a notable anodic peak associated with GMB at concentration of 0.1 mM (Fig. 3 (a)). Analysis at the same concentration does not generate this peak upon the bare carbon paste electrodes. This indicates that the AuNP upon the electrode surface are providing the enhanced electro-activity required to facilitate GMB oxidation, because of the greater electroactive surface area and

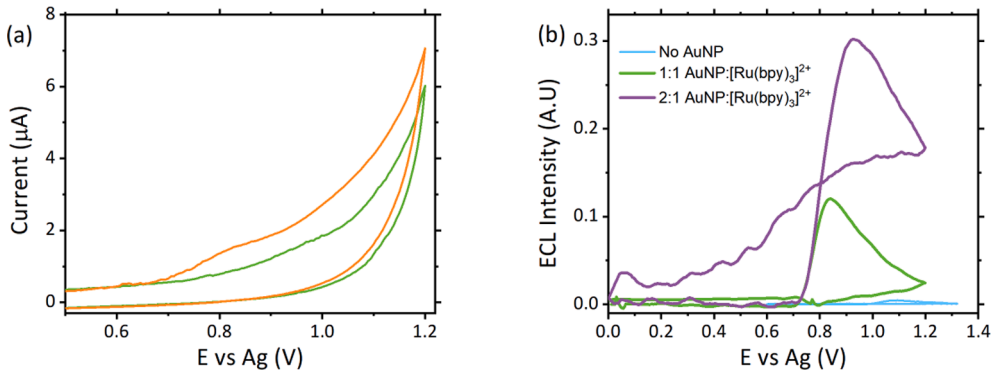

Fig. 3. (a) CV of 0.1 mM GMB upon AuNP modified carbon electrodes with a supporting electrolyte of 0.1 M NaCl (green) and (b) ECL signals obtained from AuNP:[Ru(bpy)3]2 + film electrodes with 0.1 mM GMB at a v/v ratio of AuNP to [Ru(bpy)3]2 + of 2:1 v/v (purple) and 1:1 v/v (green), compared with a ruthenium only film electrode (blue). All measurements were collected at a scan rate of 100 mV s-1 across a potential range of $0.0 \leq E \geq 1.2$ V vs. Ag with a PMT bias of 0.6 V for (b).

electrocatalytic effects associated with AuNP. As such, it was therefore envisioned that this enhanced electro-activity facilitate the generation of a recordable ECL signal from GMB with the traditional ruthenium based luminophore.

Addition of the AuNP to enhance ECL performance was achieved through their introduction into the previously optimised $[Ru(bpy)_3]^{2+}$ film. AuNP were added to the film on a volume basis, at either a 1:1 v/v ratio with 0.5 mM $[Ru(bpy)_3]^{2+}$ or 2:1 v/v ratio. Fig. 3 (b) shows the ECL signal obtained following inclusion of AuNP. Interrogation of the signal reveals a significant increase is observed in signal intensity compared the bare carbon surface. With a 60-fold and a 24-fold increase observed for the 2:1 v/v and 1:1 v/v films respectively. Despite a lower luminophore concentration, the 2:1 v/v film demonstrated the greatest enhancement effect and as such suggests the catalytic properties of the AuNP are the primary driving force in the production of ECL from GMB. We have previously reported the electrochemical mechanism observed for GMB, where we attributed the minimal ECL signal observed as a limitation of the small fraction of GMB radicals generated which can proceed down the ECL pathway [17]. This significant increase in signal intensity suggests that the catalytic properties of the AuNP promote the oxidation of GMB and hence result in a higher fraction of GMB generated radicals available. Of course, the dimerisation side reaction will still present a competing effect, however with the total number of GMB species oxidised increased the fraction available to proceed down the ECL pathway in turn also increased. The two competing reactions are shown within Scheme 1, where (c) represents the required radical for ECL generation. The radical can then proceed down one of two pathways the dimerization pathway to generate dimer (d) or the ECL pathway to regenerate GMB alongside the excited $[Ru(bpy)_3]^{2+}$ luminophore, following the energetic electron transfer between the Ru (III) species and radical (c). Hence, with a greater proportion of radical (c) present there is a higher probability that the ECL pathway will procedure, generating a detectable signal as shown within Fig. 3(b). Thus, inclusion of the AuNP enables the ability to detect GMB via the ruthenium based ECL for the first time.

3.3. *Validation of successful GMB detection via AuNP-enhanced ECL*

The marked increase in ECL signal intensity in the presence of AuNP offers an alternative detection strategy for species such as GMB who's traditional ECL detection is hindered due to competing side reactions or limited electro-activity. The increased electrocatalytic activity offered through inclusion of AuNP to the ECL film facilitated the detection of GMB down to 6.25 μM, well below the therapeutic concentration typical of this species around 26 μM [17,34]. A linear relationship was observed across a concentration range of 6.25 to 50 μM with a R^2 coefficient of 0.990 (see Fig. 4 (a)). Above 50 μM however the linear increase was lost, instead a plateau of intensity was observed. This plateau effect has been observed in a number of prior ECL systems and is a result of the $[Ru(bpy)_3]^{2+}$ complex becoming the rate limiting reagent [25,26,35–37].

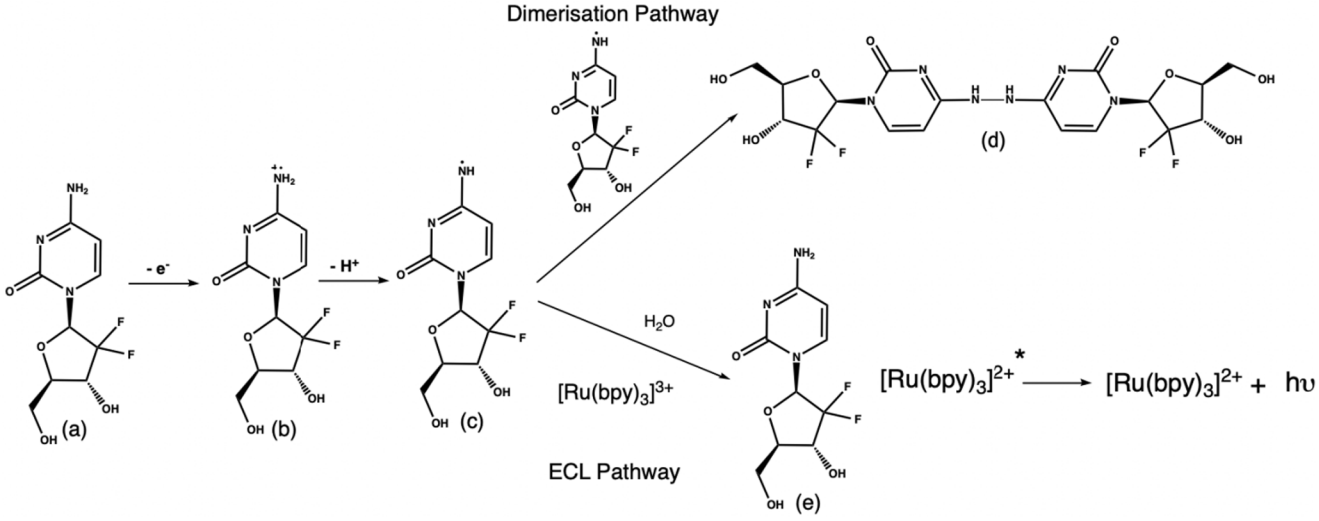

Scheme 1. Electrochemical pathway which the GMB radical can proceed down following electrocatalytic oxidation at the AuNP modified electrode surface, where (c) is the radical species, (d) is the dimerization product and (e) is the product of the ECL pathway alongside the required.

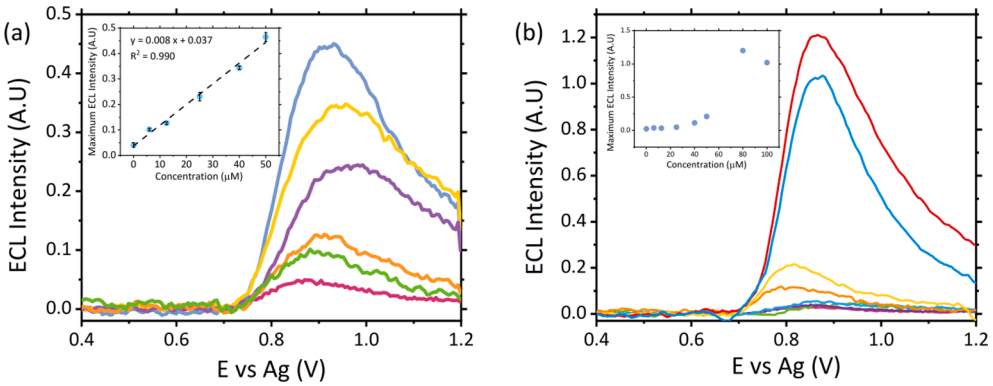

Fig. 4. ECL responses from 6.25 μM to 50 μM GMB with (a) 2:1 v/v AuNP:[Ru(bpy)3]2 + film and (b) 1:1 v/v AuNP:[Ru(bpy)3]2 + film collected at a scan rate of 100 mV s-1 across a potential range of $0.4 \leq E \geq 1.2$ V vs Ag with a PMT bias of 0.6 V. Inset shows the linear dependence between GMB concentration and maximum ECL intensity, where each point n = 3 with ± SD.

As such, no further intensity increase is observed as limited Ru(III) species remain to interact with the radical GMB molecules present. However, with the therapeutic level lying below this upper limit and the severe side effects associated with GMB administration at these concentrations, there is no clinical requirement to quantify out-with the proposed concentration range. The stability of the sensor was assessed over multiple scans (refer to Figure S3) and in-line with prior research was found that the ECL intensity decreases with subsequent scans, assigned to the irreversible oxidation of the co-reactant. Assessment was also made on the detection ranges achievable with the 1:1 v/v film to understand if the higher concentrations could be quantified via this film make-up. However, despite the increased ruthenium concentration present the lower catalytic activity offered, through a lower fraction of AuNP present, resulted in the inability to distinguish the GMB signal from the intrinsic blank signal below 40 μM (refer to Fig. 4 (b)), as such rendering this film make-up unsuitable for clinical analysis. This therefore indicates that for the development of future enhancement methods the concentration of AuNP should be prioritised over other variable factors for those species which suffer from limited ECL.

Interestingly the same enhancement effect was not observed for other species whose ECL signal with the traditional system is strong. This can be seen through consideration of the signal obtained from leucovorin (LV), a fellow cancer therapy. We have previously demonstrated the ability to reliably detect LV with the traditional $[Ru(bpy)_3]^{2+}$ luminophore below therapeutic levels with a LOD of 6.25 μM [17]. Given the 60-fold increase observed for GMB, it would be reasonable to assume that the same enhancement would be observed for LV. However as demonstrated within Fig. 5 (a), this was not the case. In fact,

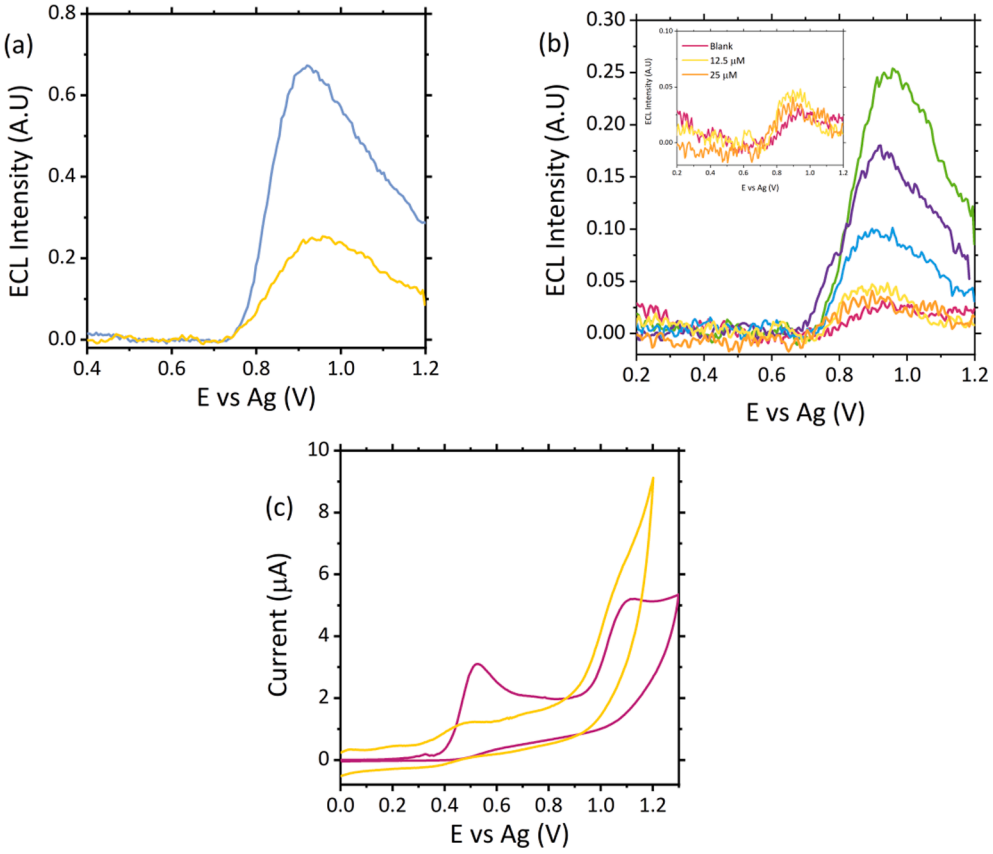

Fig. 5. (a) ECL signals recorded with 100 μM LV at a [Ru(bpy)3]2 + film electrode (purple) and 2:1 v/v AuNP: [Ru(bpy)3]2 + film electrode (yellow) and (b) ECL signals recorded from 6.25 to 100 μM LV upon 2:1 v/v AuNP: [Ru(bpy)3]2 + film electrodes, with inset highlighting the inability to distinguish therapeutically relevant concentrations from the blank. (c) CV responses for 100 μM LV upon carbon paste electrode surface (pink) and AuNP modified electrode (yellow), with 0.1 M NaCl as the supporting electrolyte, with all measurements recorded at a scan rate of 100 mV s-1 across a potential range of $0 \leq E \geq 1.25$ V vs Ag with a PMT bias for ECL measurements of 0.6 V.

comparison of the signal intensities reveals that addition of the AuNP leads to a ~ 2.8-fold decrease in intensity, resulting in the detection limit raising above the therapeutic range with no differentiation seen below 25 μM (Fig. 5 (b)). This therefore indicates that for species which readily undergo oxidation at the bare carbon electrode and hence produce ECL, will not benefit from the inclusion of AuNP. This could be related to the fact that LV can readily oxidise on the bare carbon electrode, and addition of the AuNP see's oxidation of LV reduced, see Fig. 5 (c). As such, it becomes apparent that a one size fits all enhancement approach will ultimately be unlikely with such a marked difference observed between these two species which are part of the same therapeutic group, however it may be possible that enhancement approaches could be generalised based upon a species functional group which gift it its electro-activity, this would require further investigations across a large number of species.

4. Conclusions

Within this contribution we have proven the ability to enhance the ECL signal utilising AuNP in combination with $[Ru(bpy)_3]^{2+}$ for the detection of cancer therapy drug GMB. This represents the first instance of GMB being successfully detected via ECL with the traditional ruthenium luminophore. The inclusion of AuNP into the luminophore film allowed for the oxidation of GMB to proceed upon a carbon paste electrode as a result of the electrocatalytic behaviour offered in the presence of the AuNP. By facilitating the oxidation of GMB the ECL signal intensity was increased 60-fold in comparison to that obtained with the ruthenium luminophore alone. This increased effect allowed for the detection of GMB down to 6.25 μM well within the expected therapeutic range, rendering this methodology suitable toward clinical and point-of-care devices. The ability to detect GMB in the presence of AuNP improves upon our prior publication which demonstrated the ability to utilise a different metal luminophore $(Os(diars)_2(bthp))^{2+}$) for GMB detection. However, the ability to detect it at relevant concentrations with the traditional and widely available luminophore will only promote its potential employability and simplify its introduction to those who may not have expertise in the field. Interestingly we found that the addition of AuNP does not bare the same enhancement effect across all co-reactants, finding a decrease in ECL intensity and poorer oxidation of fellow cancer therapy LV, when compared with a ruthenium only film and bare carbon electrode respectively. This bares two potential routes future routes of interest; firstly, a study investigating the various enhancement effects upon the ECL signal with the inclusion of different metallic nanoparticles and luminophore complexes should be conducted. This would provide a useful index to further the understanding between the interaction of the two different components within the system (the surface modification and ECL luminophore) leading to the enhancement or suppression effects. Secondly, an extensive investigation to ascertain which specific co-reactants would be suitable for the metallic NP enhancement effect would be beneficial. Some links could be drawn utilising the structure of proposed co-reactants, however it has been shown previously and again demonstrated here how species which structurally and thus theoretically appeared to be suitable co-reactants can indeed suffer from competing side reactions, such as the observed dimerization of GMB, rendering them unstable for ECL analysis. To this extent before ECL can be more widely adopted more understanding is required on what makes a suitable co-reactant and potential methods to overcome limitations they face, including but not limited to poor electro-activity upon a specific surface material or electrochemically initiated competing side reactions. Such findings from both aforementioned studies would be ultimately housed within an accessible open-access library to promote the expansion of this technique.

Declaration of Competing Interest

The authors declare that they have no known competing financial interests or personal relationships that could have appeared to influence the work reported in this paper.

Acknowledgements

The authors would like to thank Tenevous for financially supporting this research (S20-05).

All data underpinning this publication are openly available from the University of Strathclyde KnowledgeBase at https://doi.org/10.15129/1fdf4efb-8c0b-4d8c-8824-6c8471623522.

Appendix A. Supplementary material

Supplementary data to this article can be found online at https://doi.org/10.1016/j.bioelechem.2022.108164.

References

[1] I.R. König, O. Fuchs, G. Hansen, E. von Mutius, M.V. Kopp, Eur. Respir. J. 50 (2017) 1700391.
[2] E. Bloom, Impact of New Personalised Cancer Treatments (2018).
[3] G.R. Gameiro, V. Sinkunas, G.R. Liguori, J.O.C. Auler-Júnior, Clinics (Sao Paulo) 73 (2018) e723–e.
[4] G.S. Ginsburg, K.A. Phillips, Health Aff. (Millwood) 37 (2018) 694–701.
[5] A. Heller, B. Feldman, Chem. Rev. 108 (2008) 2482–2505.
[6] Z. Mian, K.L. Hermayer, A. Jenkins, Am. J. Med. Sci. 358 (2019) 332–339.
[7] M.M. Richter, Chem. Rev. 104 (2004) 3003–3036.
[8] W. Miao, Chem. Rev. 108 (2008) 2506–2553.
[9] E.H. Doeven, G.J. Barbante, A.J. Harsant, P.S. Donnelly, T.U. Connell, C.F. Hogan, P.S. Francis, Sens. Actuat. B 216 (2015) 608–613.
[10] M. Rizwan, N. Mohd-Naim, M. Ahmed, Sensors 18 (2018) 166.
[11] C. Ma, Y. Cao, X. Gou, J.-J. Zhu, Anal. Chem. 92 (2019) 431–454.
[12] C.K.P. Truong, T.D.D. Nguyen, I.-S. Shin, BioChip J. 13 (2019) 203–216.
[13] Y. Zhang, R. Zhang, X. Yang, H. Qi, C. Zhang, J. Pharm. Anal. 9 (2019) 9–19.
[14] P. Chandra, Sens. Int. 1 (2020) 100019.
[15] L. Hu, Y. Wu, M. Xu, W. Gu, C. Zhu, Chem. Comm. 56 (2020) 10989–10999.
[16] A. Zanut, A. Fiorani, S. Canola, T. Saito, N. Ziebart, S. Rapino, S. Rebeccani, A. Barbon, T. Irie, H.-P. Josel, Nat. Commun. 11 (2020) 1–9.
[17] K. Brown, L. Dennany, Sens. Actuat. Rep. 3 (2021) 100065.
[18] D. Mauri, N.P. Polyzos, G. Salanti, N. Pavlidis, J.P. Ioannidis, J. Natl. Cancer Inst. 100 (2008) 1780–1791.
[19] Y. Wang, Y. Kuramitsu, K. Tokuda, B. Baron, T. Kitagawa, J. Akada, S.-I. Maehara, Y. Maehara, K. Nakamura, PLoS One 9 (2014) e109076.
[20] L. de Sousa Cavalcante, G. Monteiro, Eur. J. Pharmacol. 741 (2014) 8–16.
[21] A.J. Lightfoot, B. N. Breyer, H. M. Rosevear, B. A. Erickson, B. R. Konety, M. A. O'Donnell, presented in part at the Urologic Oncology: Seminars and Original Investigations, 2014.
[22] S.S. Kalanur, U. Katrahalli, J. Seetharamappa, J. Electroanal. Chem. 636 (2009) 93–100.
[23] K.M. Naik, S.T. Nandibewoor, J. Ind. Eng. Chem. 19 (2013) 1933–1938.
[24] A. Florea, Z. Guo, C. Cristea, F. Bessueille, F. Vocanson, F. Goutaland, S. Dzyadevych, R. Săndulescu, N. Jaffrezic-Renault, Talanta 138 (2015) 71–76.
[25] K. Brown, M. McMenemy, M. Palmer, M.J. Baker, D.W. Robinson, P. Allan, L. Dennany, Anal. Chem. 91 (2019) 12369–12376.
[26] K. Brown, C. Gillies, P. Allan, L. Dennany, Electrochim. Acta 372 (2021) 137885.
[27] Q.-Q. Gai, D.-M. Wang, R.-F. Huang, X.-X. Liang, H.-L. Wu, X.-Y. Tao, Biosens. Bioelectron. 118 (2018) 80–87.
[28] Y. Zu, A.J. Bard, Anal. Chem. 73 (2001) 3960–3964.
[29] Z. Chen, Y. Zu, J. Phys. Chem. B 113 (2009) 21877–21882.
[30] Z. Chen, Y. Zu, Langmuir 23 (2007) 11387–11390.
[31] Y.-P. Dong, H. Cui, Y. Xu, Langmuir 23 (2007) 523–529.
[32] S. Xu, Y. Liu, T. Wang, J. Li, Anal. Chem. 82 (2010) 9566–9572.
[33] M. Tominaga, T. Shimazoe, M. Nagashima, H. Kusuda, A. Kubo, Y. Kuwahara, I. Taniguchi, J. Electroanal. Chem. 590 (2006) 37–46.
[34] J. Ciccolini, C. Serdjebi, G.J. Peters, E. Giovannetti, Cancer Chemother. Pharmacol. 78 (2016) 1–12.
[35] K. Brown, C. Jacquet, J. Biscay, P. Allan, L. Dennany, Anal. Chem. 92 (2020) 2216–2223.
[36] Z. Mohsan, A.L. Kanibolotsky, A.J. Stewart, A.R. Inigo, L. Dennany, P.J. Skabara, J. Mater. Chem. C 3 (2015) 1166–1171.
[37] A.J. Stewart, K. Brown, L. Dennany, Anal. Chem. 90 (2018) 12944–12950.